Geometric Perfusion Deficits: A Novel OCT Angiography Biomarker for Diabetic Retinopathy Based on Oxygen Diffusion

SIYU CHEN, ERIC M. MOULT, LINDA M. ZANGWILL, ROBERT N. WEINREB, AND JAMES G. FUJIMOTO

• PURPOSE: To develop geometric perfusion deficits (GPD), an optical coherence tomography angiography (OCTA) biomarker based on oxygen diffusion, and to evaluate its utility in a pilot study of healthy subjects and patients with diabetic retinopathy (DR).

• DESIGN: Retrospective cross-sectional study.

• METHODS: Commercial spectral-domain optical coherence tomography angiography (OCTA) instruments were used to acquire repeated 3 × 3-mm^2 and 6 × 6-mm^2 motion-corrected macular OCTA volumes. En face OCTA images corresponding to the superficial capillary plexus (SCP), deep capillary plexus (DCP), and full retinal projections were obtained using automatic segmentation. For each projection, the GPD percentage and the vessel density percentage, the control metric, were computed, and their values were compared between the normal and DR eyes. The repeated OCTA acquisitions were used to assess the test-retest repeatability of the GPD and vessel density percentages.

• RESULTS: Repeated OCTA scans of 15 normal eyes and 12 DR eyes were obtained. For all en face projections, GPD percentages were significantly higher in DR eyes than in normal eyes; vessel density percentages were significantly lower in all but 1 projection (DCP). Large GPD areas were used to identify focal perfusion deficits. Test-retest analysis showed that the GPD percentage had superior repeatability than the vessel density percentage in most cases. A strong negative correlation between the GPD percentage and the vessel density percentage was also found.

• CONCLUSIONS: Geometric perfusion deficits, an OCTA biomarker based on oxygen diffusion, provides a quantitative metric of macular microvascular remodeling with a strong physiological underpinning. The GPD percentage may serve as a useful biomarker for detecting and monitoring DR. (Am J Ophthalmol 2021;222:256–270. © 2020 Elsevier Inc. All rights reserved.)

DIABETIC RETINOPATHY (DR) IS A COMMON ocular complication of diabetes mellitus and a leading cause of visual impairment in adults. In its early, nonproliferative DR (NPDR) stage, hyperglycemia and pericyte loss can lead to microvasculature remodeling (eg, microaneurysms, capillary dropout, and macular nonperfusion).[1,2] Subsequent deterioration of vascular function exacerbates retinal ischemia, further driving abnormal vessel growth and leading to the late proliferative DR stage (PDR).[2,3] DR patients often experience few symptoms prior to sudden, and potentially irreversible, vision loss, which motivates the need for screening and monitoring strategies that can be implemented during routine clinical visits.

Due to its importance, there is substantial medical literature investigating vascular alterations in DR. Early investigations used fluorescein angiography to study DR-associated vascular alterations. Although the utility of fluorescein angiography for staging DR has been established,[4,5] the need for exogeneous contrast (dye) injection constrains its usage. In the past decade, optical coherence tomography angiography (OCTA), a functional extension of OCT, has emerged as a promising modality for visualizing ocular microvasculature.[6,7] Unlike fluorescein angiography, OCTA is noninvasive and uses flowing blood cell motion rather than fluorescent dye to generate vascular contrast. This, combined with its high-resolution, short imaging times, and depth resolvability has made OCTA a well-suited modality for studying vascular alterations in DR.

A variety of metrics have been proposed for detecting and staging DR by using en face OCTA images, including OCTA vessel density[8–12] and its complement, nonperfusion area.[13–17] These early studies used manual segmentation or simple thresholding to identify retinal vessels and demarcate nonperfused areas. Later, automatic segmentation algorithms were developed to extract vascular features such as intercapillary areas.[16,17] Notably, Krawitz and associates[16] demarcated parafoveal intercapillary areas by using threshold levels derived from normal eyes, revealing both global and focal vascular changes during DR progression. However, intercapillary area analysis is particularly sensitive to segmentation

Accepted for publication Sep 2, 2020.

From the Department of Electrical Engineering and Computer Science, and Research Laboratory of Electronics (S.C., E.M.M., J.G.F.), Massachusetts Institute of Technology, Cambridge, Massachusetts, USA; and the Hamilton Glaucoma Center (L.M.Z., R.N.W.), Viterbi Family Department of Ophthalmology and the Shiley Eye Institute, University of California, San Diego, San Diego, California, USA.

Inquiries to James G. Fujimoto, Department of Electrical Engineering and Computer Science, and Research Laboratory of Electronics, Massachusetts Institute of Technology, 77 Massachusetts Ave, Cambridge, MA 02139, USA; e-mail: jgfuji@mit.edu

0002-9394/$36.00
https://doi.org/10.1016/j.ajo.2020.09.007

errors, and high signal-to-noise ratio OCTA images are required.[16,17] Although averaging multiple OCTA volumes can increase signal-to-noise ratio,[18] it also extends imaging times, which is not always feasible in clinical settings. Furthermore, although intercapillary area analysis has shown promising correlation with DR severity, there has been little physiological rationale for choosing particular intercapillary area thresholds, which complicates interpretation and motivates the need for normative databases.

Noting the limitations of existing metrics, this study defined and developed geometric perfusion deficits (GPD), a novel OCTA metric based on oxygen diffusion that is computed using microvascular geometry. This study then presented evaluation of the GPD framework for its test-retest repeatability, as well as pilot results of assessing microvascular remodeling in DR eyes.

METHODS

• **PATIENT RECRUITMENT:** This retrospective, cross-sectional study used OCTA data obtained as part of a larger repeatability and reproducibility study of OCTA imaging at the Shiley Eye Institute, University of California, San Diego (USCD; San Diego, California, USA). The respective Institutional Review Boards at UCSD and Massachusetts Institute of Technology approved the study protocol. All procedures performed adhered to the tenets of the Declaration of Helsinki and complied with the Health Insurance Portability and Accountability Act of 1996.

We identified healthy normal, and DR subjects who underwent multiple OCTA imaging procedures during a single visit over a one-half year period (August 2016 to January 2017). Diabetic retinopathy was classified for each subject using the Early Treatment Diabetic Retinopathy Study (ETDRS) standard grading protocols as mild, moderate, or severe NPDR or as PDR.[19] The presence or absence of diabetic macular edema (DME) was based on structural OCT findings.

• **OCTA ACQUISITION AND PROCESSING:** All subjects underwent repeated OCTA acquisitions during a single visit, using the AngioVue SD-OCT instrument (Optovue, Fremont, California, USA). Only 1 eye was imaged for each subject. The imaging session had a sequence of scanning protocols (ie, $3 \times 3\text{-mm}^2$ and $6 \times 6\text{-mm}^2$ OCTA centered at the fovea and $3 \times 3\text{-mm}^2$ and $6 \times 6\text{-mm}^2$ OCTA centered at the optic disk). This sequence was then repeated 2 to 4 times. Between scanning protocols, subjects were allowed to rest, and the instrument was readjusted as required. Thus, the time between 2 identical scanning protocol repeats was approximately 5-10 minutes. To generate motion-corrected OCTA volumes, 2 volumetric OCTA scans with orthogonal horizontal-priority and vertical-priority rasters were obtained in quick succession.[20–22] Optovue motion correction technology was then used to register and merge the 2 orthogonal scans, creating a single OCTA scan with reduced motion artifacts and improved signal-to-noise contrast.

Motion-corrected $3 \times 3\text{-mm}^2$ and $6 \times 6\text{-mm}^2$ macular OCTA scans were analyzed from normal and DR eyes. The $3 \times 3\text{-mm}^2$ scans consisted of 304×304 A-lines, whereas the $6 \times 6\text{-mm}^2$ scans had 400×400 A-lines. Comparing the 2 protocols, the $6 \times 6\text{-mm}^2$ scans had roughly 50% reduced sampling density and approximately 70% longer acquisition time. This reduces OCTA quality perceptibly and can impact subsequent quantitative analyses. Image quality for larger scans is also a concern in other OCTA vessel density studies.[8,9] Thus, most of this study's quantitative analyses used the smaller $3 \times 3\text{-mm}^2$ field of view scans, whereas the test-retest repeatability and intergroup statistical tests were also evaluated using $6 \times 6\text{-mm}^2$ scans.

The automatic segmentation and projection algorithms of the AngioVue ReVue software were used to generate en face OCTA images of the superficial capillary plexus (SCP), the deep capillary plexus (DCP), and the full retinal OCTA projections for both OCTA fields. Specifically, the SCP projection is generated by axially projecting the OCTA volume between the inner limiting membrane and the posterior boundary of the inner plexiform layer. The DCP projection is generated by axially projecting the OCTA volume between the posterior boundary of the inner plexiform layer and the posterior boundary of the outer plexiform layer; and the full retinal projection, which contains both the SCP and the DCP, is generated by axially projecting the OCTA volume between the inner limiting membrane to the outer boundary of the outer plexiform layer.

• **GEOMETRIC PERFUSION DEFICITS:** The GPD identifies regions of retinal tissue that are inadequately perfused as a result of alterations in vessel geometry (eg, vascular dropout, displacement, tortuosity). In computing GPD, the underlying hypothesis is that, because diffusing oxygen is consumed as it passes through retinal tissue, the concentration of oxygen decreases as the distance from the supplying capillaries increases. Thus, if the supplying capillaries are far from a given retinal cell, that cell will be inadequately perfused and, therefore, in an ischemic condition.

This hypothesis suggests a 2-step approach for computing the GPD: first, for each nonvessel pixel, the capillary perfusion distance, that is, the minimum distance that an oxygen molecule must diffuse to reach that pixel, is computed; and, second, based on this distance, the pixel is classified as either adequately or inadequately perfused. All computations were performed using MATLAB version R2017a software (MathWorks, Natick, Massachusetts, USA).

Computing the Capillary Perfusion Distance. When the capillary perfusion distance is computed, it is assumed

that i) oxygen diffuses along the 2-dimensional (2D) en face plane defined by the OCTA projection (ie, the SCP, DCP, or full retinal projections); and ii) that for each nonvessel pixel, the capillary perfusion distance is equal to the distance between that pixel and the nearest vessel pixel. Although this assumption is clearly a simplification of the actual oxygen diffusion mechanism, prior studies of retinal oxygen tension using animal models strongly suggest oxygen molecules predominantly diffuse transversely within the inner retina, at least in light-adapted retina and under normoxic conditions.[23–26]

Building on a prior OCTA intercapillary area scheme,[17] the following algorithm calculates capillary perfusion distance as follows. First, a 3-stage OCTA filtering routine is performed, which consists of: i) an adaptive filter normalizes the input OCTA image contrast to a consistent gray-scale range; ii) a Frangi vesselness filter to emphasize vascular features and suppress noise[27]; and iii) a second application of the normalization filter. Together, these filtering steps improve the consistency of subsequent vessel segmentation and skeletonization wherein the identified vessels are reduced to a single pixel in width. Analyzing the skeletonized vessels has the advantage of reducing blurring, which can be caused by residual refractive error or uncorrected motion artifacts.[8] However, by reducing the vessel width to a single pixel, skeletonization replaces the lumens of larger retinal vessels with an artifactual "vessel-free" zone. To mitigate this artifact, a binary mask of the large retinal vasculature was generated and excluded these larger vessel areas from the analysis. As the final step, the linear (Euclidean) distance between each nonvessel pixel and the closest vessel skeleton was calculated, generating an en face "capillary perfusion map."

Identifying Geometric Perfusion Deficits. GPDs are identified by thresholding the capillary perfusion distance map obtained in the previous step. In this study, the distance threshold was 30 μm, that is, pixels with the nearest vessel skeleton greater than 30 μm away are considered geometric perfusion deficits. The 30-μm threshold was selected using data from prior studies of parafoveal intercapillary distances, which used adaptive optics scanning laser ophthalmoscope, laser Doppler flowmetry, and OCTA.[16,28,29]

It is important to note that the foveal avascular zone (FAZ) would also satisfy this definition of perfusion deficits. However, the FAZ was excluded from the calculation of GPD for 2 reasons. First, the FAZ is a normal physiological feature of the healthy retina and, thus, does not represent a pathological nonperfusion. Second, previous studies have shown that the FAZ demonstrated morphological alterations during DR progression.[16,30–32] Because this study focuses on investigating whether pathological perfusion defects are indicative of DR, it was decided not to include the FAZ in these metrics.

To mitigate variations in field of view among scans, the total areas of identified perfusion deficits were normalized to yield a percentage value, analogous to the percentage value reported by the vessel density metric. For the 3 × 3-mm^2 OCTA scans, the reference area was defined as the annulus between the 1-mm-diameter and 3-mm-diameter circles in the ETDRS grid. In the 6 × 6-mm^2 OCTA scans, the parafoveal, perifoveal, and combined para- and perifoveal regions were chosen as references. The boundaries of those annuli are demarcated by the corresponding ETDRS grids (parafoveal, 1-mm- and 3-mm-diameter circles; perifoveal, 3-mm- and 6-mm-diameter circles; and combined para- and perifoveal, 1-mm- and 6-mm-diameter circles). Areas that belonged to the FAZ, as well as those covered by the vascular mask, were excluded. The following formula was used for calculating the GPD percentage

$$\text{GPD Percentage} = \frac{(\text{Total Perfusion Deficit Area})}{(\text{Total Reference Area})} \times 100\%.$$

Additionally, the sum of the 10 and 20 largest GPD areas within the same reference areas were calculated to investigate their respective performance as markers for focal lesions.

• **VESSEL DENSITY PERCENTAGE AS A CONTROL METRIC:** The vessel density percentage, which measures the percentage of vessel pixels of a given retinal region, was used as a control metric with which to compare the GPD percentage. The vessel density percentage was chosen because i) it is a commonly used metric in OCTA imaging studies; and ii) a US Food and Drug Administration-approved, standardized implementation is available on the OCT instruments (Optovue). The vessel density percentage was retrieved from the AngioVue ReVue software (Optovue) in the same ETDRS grid regions as for the GPD analysis.

• **STATISTICAL ANALYSIS:** Statistical analysis was performed using Excel software (Microsoft, Redmond, Washington, USA) and MATLAB version R2017a software (MathWorks). To verify the repeatability of the GPD and vessel density percentage, the standard deviations (SD) of both metrics were calculated from repeated OCTA acquisitions. Because both metrics use an interval percentage scale, the metrics were not normalized by their respective means to generate coefficient of variance (COV). Additionally, the different spans of GPD and vessel density percentages prevented direct comparison of COV between the 2 metrics. Thus, the SD, instead of COV, was used as the statistic for characterizing and comparing the consistency of GPD and vessel density percentages. The differences in SD of repeated measurements were tested using unpaired Wilcoxon rank-sum significance tests (*U*-test).

Intraclass correlation coefficients were also calculated to characterize the consistency of repeated measurements (ie, test-retest repeatability) in the context of

TABLE 1. Subject Demographics

Group	Males:Females	Number with DME	Age[a]	*P* Value[b]
Normal	3:12	-	47 ± 22 (19-84)	-
Total DR	3:9	9	56 ± 13 (31-77)	.25
NPDR	2:4	5	64 ± 10 (52-77)	.09
PDR	1:5	4	48 ± 10 (31-58)	1.00

DME = diabetic macular edema; DR = diabetic retinopathy; NPDR = nonproliferative diabetic retinopathy; PDR = proliferative diabetic retinopathy; SD = standard deviation.

[a]Data are mean ± SD in years (range).

[b]Significance level is $P < .05$. *P* values are respectively calculated against the normal category using unpaired Student *t*-tests.

DR-induced vascular remodeling using a 2-way mixed effects model.[33]

Intergroup statistical tests using the global GPD percentage, global vessel density percentage, and focal GPD areas were carried out as follows. First, for each eye, the mean values of each metric from repeated OCTA acquisitions were assigned to each eye. Second, nonparametric Kruskal-Wallis 1-way analysis of variance of grouped GPD and vessel density metrics was performed. Third, when appropriate, a post hoc Dunn test, corrected for multiple comparison, was used to compare among normal eyes, eyes diagnosed with NPDR and PDR eyes.[34]

Finally, the correlation between the GPD percentage and vessel density percentage was assessed by performing a linear regression and computing the Pearson correlation coefficients between the 2.

RESULTS

• **SUBJECT DEMOGRAPHICS:** A total of 27 subjects (15 healthy controls and 12 with DR) were retrospectively identified. Table 1 summarizes the demographic information of the subjects included in this study. Due to the small cohort size, the 1 mild NPDR eye and 5 moderate NPDR eyes were combined into a single NPDR group for subsequent analyses. Moreover, eyes with and without DME were not segregated for the purposes of intergroup statistical tests. Using unpaired Student *t*-tests, it was found there were no significant differences in age among the normal, NPDR, and PDR groups.

• **STABILITY AND SENSITIVITY ADVANTAGE OF GEOMETRIC PERFUSION DEFICITS:** While GPD analysis is conceptually related to vessel density and intercapillary area analysis, it overcomes some major limitations of these metrics. Most notably, GPD, and its underlying capillary perfusion distance intermediate, are robust against OCTA imaging artifacts, sensitive to focal changes, and directly physiologically interpretable.

Figure 1 illustrates these improvements by comparing the similarities and differences among capillary perfusion distances, the intercapillary areas, and the vessel densities. In Figure 1, capillary perfusion distances, intercapillary areas, and vessel densities are calculated on a sample skeletonized retinal capillary network, respectively. From Figure 1, it is evident that longer capillary perfusion distances coincide with larger intercapillary areas. However, unlike intercapillary areas, perfusion distances are robust against vessel discontinuities, which commonly occur in OCTA because of a variety of causes, including speckle noise, stochastic blood flow, and motion artifacts. In particular, vessel discontinuities can cause intercapillary areas to merge, creating a single, artificially enlarged area (Figure 1, left column).[17] In contrast, such artifacts cause only minor alterations in the perfusion distance map (Figure 1, middle plot). Thus, it is reasonable to expect that the subsequent GPD analysis will not be affected significantly, where the intercapillary analysis can have pronounced overestimations. The comparison also demonstrates the fact that vessel density cannot proportionately detect certain focal vessel remodeling as capillary perfusion analysis does (Figure 1, center-bottom plot). In fact, both the vessel length density and area density will remain mostly unchanged in this hypothetical case (Figure 1, right column).

• **QUALITATIVE EVALUATION ON GEOMETRIC PERFUSION DEFICITS AND VESSEL DENSITY:** Figure 2 shows representative en face capillary perfusion distance and vessel density maps for SCP, DCP, and full retinal OCTA projections from 3 × 3-mm^2 macular scans. In the capillary perfusion distance maps (Figure 2 rows 1, 3, and 5), pixels with perfusion distances greater than 30 μm are highlighted and color-coded. The corresponding vessel density maps (Figure 2, rows 2, 4, and 6) are retrieved from the AngioVue ReVue software. The 2 normal eyes of similar age as the NPDR and PDR eyes are respectively selected. Visual inspection reveals that both DR eyes have larger and more frequent patches of areas with long capillary perfusion distances. This is most evident in the SCP OCTA projection. Additionally, the increased perfusion distances coincide with reduced vessel density, as indicated by the blue hue in vessel density maps.

• **QUANTITATIVE GEOMETRIC PERFUSION DEFICITS AND VESSEL DENSITY ANALYSIS USING 3 × 3-MM² MACULAR OCTA:** All but 2 subjects had 3 repeated 3 × 3-mm^2 OCTA scans. One normal subject had 2 repeated OCTA scans, and another normal subject had 4 repeated scans.

Test-Retest Repeatability. Figure 3 plots GPD percentage and vessel density percentage for each subject using the SCP, DCP, and full retinal OCTA from repeated 3 × 3-

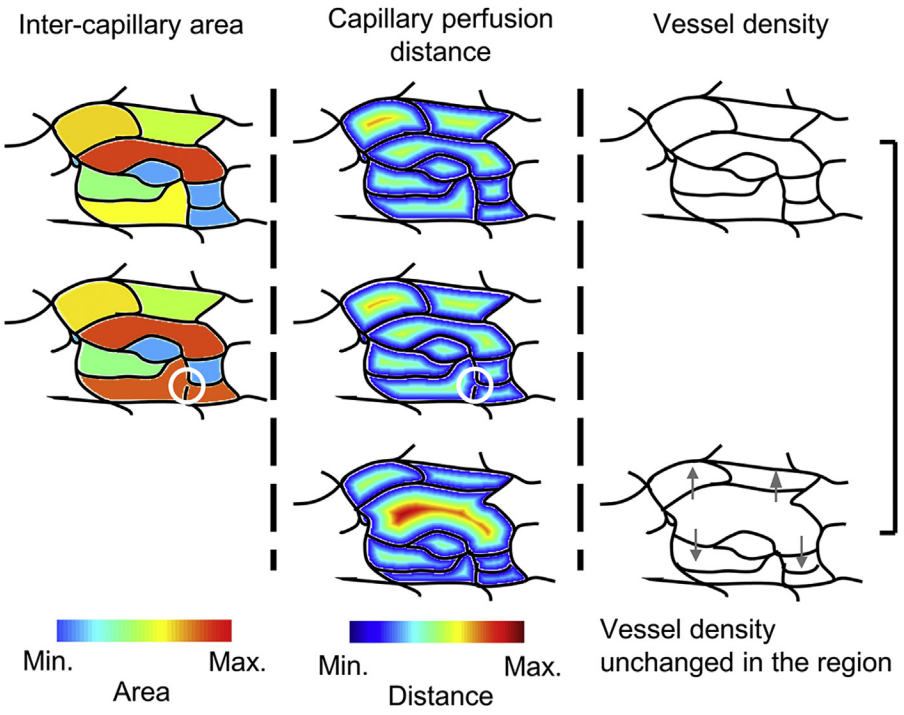

FIGURE 1. Schematic of a skeletonized capillary network. (Top row) Ground truth network. (Middle row) The same network but with an artifactual discontinuity (white circle). In the intercapillary area analysis (left column), the discontinuity leads to the merging of 2 adjacent regions into a single, markedly enlarged intercapillary area. In contrast, the effect of this discontinuity is insignificant in the perfusion distance map (middle plot). (Bottom row) Hypothetical focal lesion characterized by displaced vessels. The vessel density analysis will not detect this hypothetical lesion, as the linear or area vessel density remains mostly unchanged for the region (right column); however, the capillary perfusion distance analysis proportionately detects these focal lesions (center-bottom plot).

mm^2 macular scans. The vertical axes are scaled so that they cover the same percentage range to allow intuitive comparison between the two metrics.

Mean and median standard deviations for repeated GPD percentage and vessel density percentage measurements are summarized in Table 2. All repeated measurements of GPD percentage have significantly lower standard deviations than repeated vessel density percentage measurements, except for the SCP projection in DR subjects. The intraclass correlation coefficients for both GPD and vessel density percentages show good intragroup test-retest repeatability (Table 3).

Global Geometric Perfusion Deficits and Vessel Density Changes in Diabetic Retinopathy. Global GPD percentage can be used as a biomarker for identifying DR eyes in a fashion similar to that of vessel density percentage, an established OCTA vascular marker in DR research.[8,9] Figure 4 summarizes 3 × 3-mm^2 GPD and vessel density percentages for all study eyes. Intergroup statistics are listed in Table 4. For all OCTA projections, both NPDR and PDR eyes have significantly increased GPD percentages compared to normal eyes. There are no statistically significant differences in the GPD percentages between the NPDR and PDR groups.

For all OCTA projections, except for DCP, NPDR and PDR eyes have significantly decreased vessel density percentages compared to normal eyes. There are no statistically significant differences in the vessel density percentages between the NPDR and PDR groups.

To investigate the impact of OCTA imaging quality, analysis was repeated and excluded lower quality OCTA scans, particularly OCTA images with quality index <5, as reported by the AngioVue ReVue software. In total, 3 OCTA images from 3 normal subjects, 6 OCTA images from 3 NPDR subjects, and 3 OCTA images from 1 PDR subject were excluded. The exclusion led to a decrease of 1 subject in the NPDR and PDR categories, respectively. Figure 5 and Table 5 summarize the results for both GPD percentage and vessel density percentage metrics. Generally, our conclusions held when performing the analysis using only quality index ≥5 OCTA images. In most of the analyses, *P* values became less significant because of the smaller sample size and reduced statistical power; however, the difference in DCP vessel density percentage between normal and PDR groups became significant.

Focal Geometric Perfusion Deficits Changes in Diabetic Retinopathy. In addition to computing a global percentage, it is also straightforward to analyze geometric perfusion

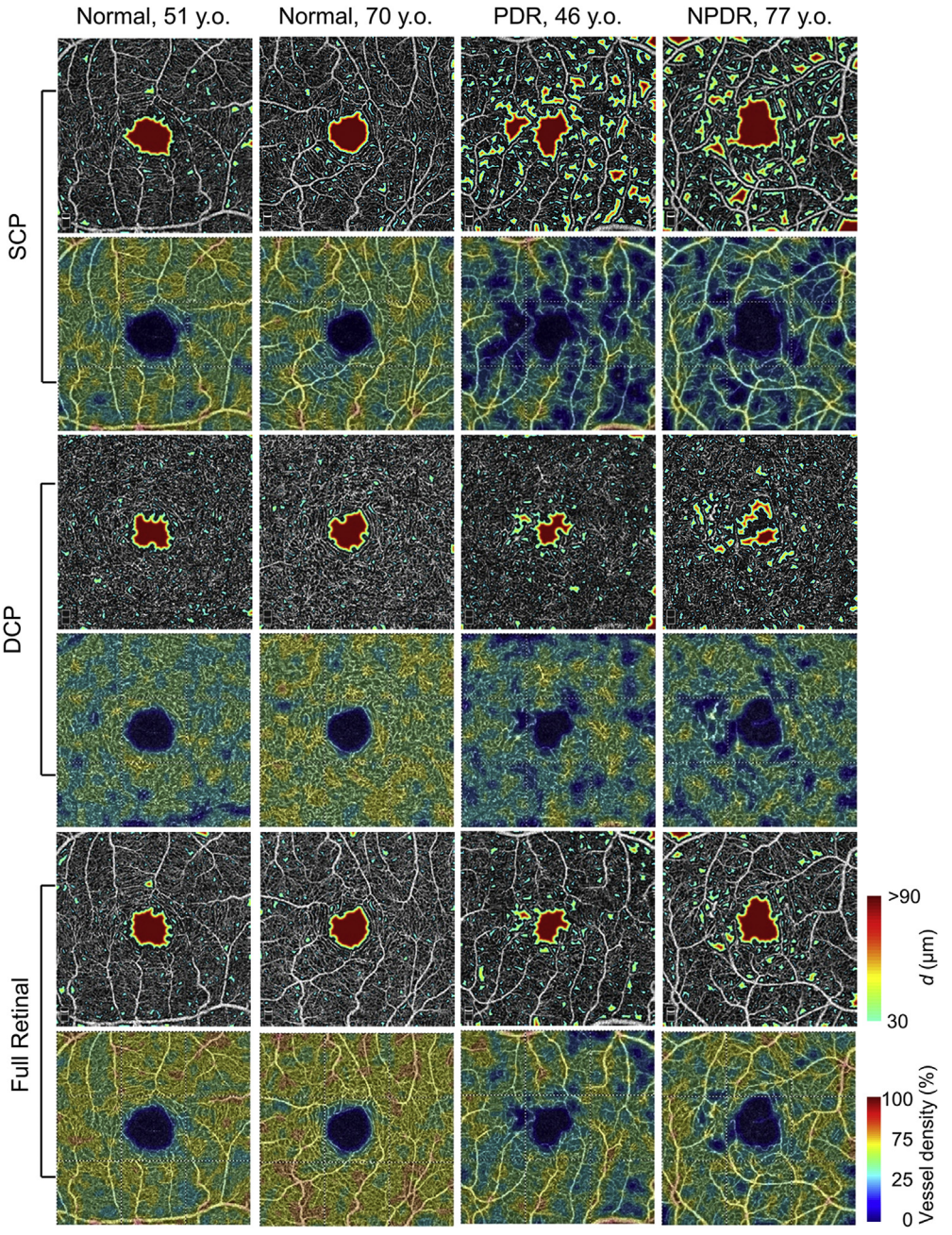

FIGURE 2. Representative capillary perfusion distance and vessel density maps of 4 representative subjects, generated by using SCP, DCP, and full retinal OCTA projections from 3 × 3-mm^2 macular scans, respectively. (Rows 1, 3, and 5) Perfusion distance maps. GPD areas (where capillary perfusion distance *d* was > 30 μm) and FAZ are highlighted using pseudocolor based on capillary perfusion distance. (Rows 2, 4, and 6) Vessel density maps retrieved from Optovue software. DCP = deep capillary plexus; FAZ = foveal avascular zone; GPD = geometric perfusion deficit; OCTA = optical coherence tomography angiography; SCP = superficial capillary plexus.

deficits individually, identifying focal vascular alterations. To perform such a focal analysis, the sum of the 10 and 20 largest GPD areas was computed and summarized in Table 6 and Figure 6. Similar to the GPD percentage, NPDR and PDR eyes show a significant increase in the focal GPD areas compared to normal eyes (Table 7). In contrast, there is no straightforward approach to assess focal changes using the vessel density metric.

Correlation between the Geometric Perfusion Deficits and Vessel Density Metrics. Figure 7 shows linear regression plots for the GPD percentage versus the vessel density

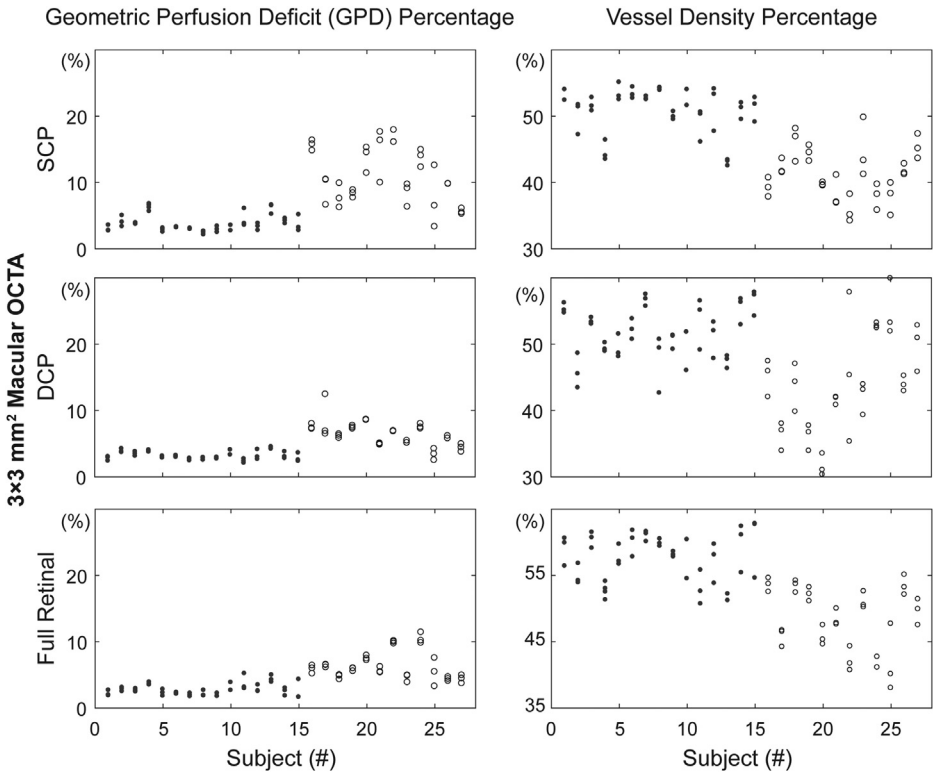

FIGURE 3. Scatter plots show repeated measurements of GPD percentages and vessel density percentages for each subject by using SCP, DCP, and full retinal OCTA projections from 3 × 3- mm^2 macular scans. Filled circles = normal eyes; open circles = eyes diagnosed with diabetic retinopathy. DCP = deep capillary plexus; GPD = geometric perfusion deficit; OCTA = optical coherence tomography angiography; SCP = superficial capillary plexus.

TABLE 2. Mean and Median SD of Repeated Measurements for GPD and Vessel Density Percentages Using 3 × 3-mm^2 Macular OCTA Scans

		GPD Percentage		Vessel Density Percentage		*P* Value[a]
Group	OCTA Projection	Mean SD	Median SD	Mean SD	Median SD	(*U* test)
Normal	SCP	0.54	0.48	1.37	1.28	.004
	DCP	0.33	0.30	2.02	1.84	< .001
	Full Retinal	0.54	0.46	2.03	1.63	< .001
DR	SCP	1.74	1.57	1.91	1.91	.40
	DCP	0.56	0.27	3.01	2.30	< .001
	Full Retinal	0.59	0.42	1.66	1.36	< .001

DCP = deep capillary plexus; DR = diabetic retinopathy; GPD = geometric perfusion deficits; OCTA = optical coherence tomography angiography; SCP = superficial capillary plexus; SD = standard deviation.

[a]Significance level is $P < .05$. Wilcoxon rank-sum significance test (*U* test) was used to compare the median standard deviations of the geometric perfusion deficit and vessel density percentages.

TABLE 3. ICC from Repeated GPD and Vessel Density Percentage Measurements Using 3 × 3-mm^2 Macular OCTA Scans

	GPD Percentage		Vessel Density Percentage	
OCTA Projection	ICC	95% CI	ICC	95% CI
SCP	0.89	0.79-0.95	0.93	0.86-0.97
DCP	0.86	0.74-0.94	0.78	0.60-0.90
Full Retinal	0.94	0.88-0.97	0.93	0.86-0.97

CI = confidence interval; DCP = deep capillary plexus; GPD = geometric perfusion deficits; ICC = intraclass correlation coefficient; OCTA = optical coherence tomography angiography; SCP = superficial capillary plexus.

percentage from the SCP, DCP, and full retinal OCTA projections. The Pearson correlation coefficients are −0.91 (95% confidence interval [CI], −0.96 to −0.81); −0.78 (95% CI: −0.89 to −0.57); and −0.89 (95% CI: −0.95 to −0.78) for the SCP, DCP, and full retinal OCTA projections, respectively.

• **QUANTITATIVE GEOMETRIC PERFUSION DEFICITS AND VESSEL DENSITY ANALYSIS USING 6 × 6-MM^2 MACULAR OCTA:** All but 2 subjects had 3 repeated 6 × 6-mm^2 OCTA scans; 1 normal subject had 2 repeated OCTA scans, and another normal subject had 4 scans. The subjects

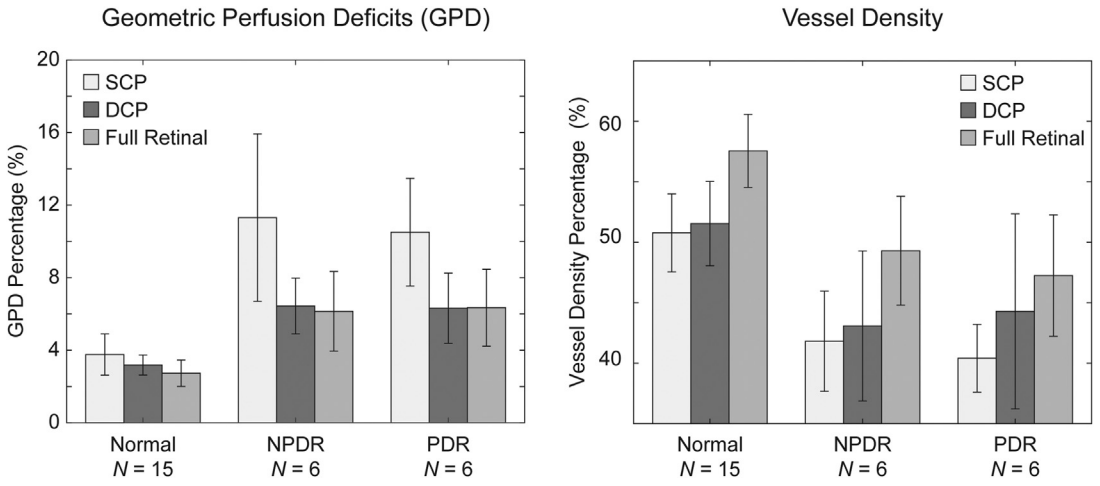

FIGURE 4. Bar plot shows GPD percentage and vessel density percentage calculated using SCP, DCP, and full retinal OCTA projections, respectively. Eyes are subdivided into 3 groups: normal, NPDR, and PDR. All 3 × 3-mm^2 macular OCTA scans are included. DCP = deep capillary plexus; GPD = geometric perfusion deficit; NPDR = nonproliferative diabetic retinopathy; PDR proliferative diabetic retinopathy; OCTA = optical coherence tomography angiography; SCP = superficial capillary plexus.

TABLE 4. GPD Percentage, Vessel Density Percentage, and Statistical Significance (*P* values) for Differentiating Normal Eyes and Eyes with Diabetic Retinopathy (All 3 × 3-mm^2 Macular OCTA Scans)

	GPDs			Vessel Density		
	SCP	DCP	Full Retinal	SCP	DCP	Full Retinal
Percentage[a]						
Normal (n = 15)	3.8 ± 1.1	3.2 ± 0.6	2.7 ± 0.7	50.8 ± 3.2	51.5 ± 3.5	57.6 ± 3.0
NPDR (n = 6)	11.3 ± 4.6	6.4 ± 1.5	6.1 ± 2.2	41.8 ± 4.1	43.1 ± 6.2	49.3 ± 4.5
PDR (n = 6)	10.5 ± 3.0	6.3 ± 1.9	6.3 ± 2.1	40.4 ± 2.8	44.3 ± 8.1	47.2 ± 5.0
P value[b]						
Normal vs. PDR	.002	.002	.002	.01	.02	.01
Normal vs. PDR	.002	.004	.001	.001	.09	.002
NPDR vs. PDR	1.00	1.00	1.00	1.00	1.00	1.00

DCP = deep capillary plexus; GPD = geometric perfusion deficit; NPDR = nonproliferative diabetic retinopathy; OCTA = optical coherence tomography angiography; PDR = proliferative diabetic retinopathy; SCP = superficial capillary plexus.

[a]Data are mean ± standard deviation.

[b]Significance level is $P < .05$. *P* values were calculated using Kruskal-Wallis 1-way ANOVA on ranks and post hoc Dunn tests corrected for multiple comparison ($m = 3$).

who received 2 or 4 repeated 6 × 6-mm^2 scans were not the same ones who received 2 or 4 repeated 3 × 3-mm^2 scans.

This study presents 6 × 6-mm^2 GPD and vessel density quantifications using the SCP OCTA projection only. This is primarily due to image quality limitations for the DCP OCTA; and the 3 × 3-mm^2 results indicated that SCP OCT projection provided most repeatable and sensitive quantification performances for both GPD and vessel density metrics.

Test-Retest Repeatability (6 × 6-mm^2). Figure 8 plots GPD percentage and vessel density percentage from the parafoveal, perifoveal, and combined para- and perifoveal regions, respectively. The combined para- and perifoveal vessel density percentages are not reported by the AngioVue ReVue software and, thus, were not shown. Similar to the 3 × 3-mm^2 test-retest repeatability results, it was found all repeated measurements of GPD percentage have significantly lower SDs than repeated vessel density percentage measurements in both parafoveal and perifoveal regions (Table 8).

Global Geometric Perfusion Deficits and Vessel Density Changes in Diabetic Retinopathy (6 × 6-mm^2). Both GPD and vessel density percentages calculated using the 6 × 6-mm^2 SCP OCTA demonstrated similar relationships

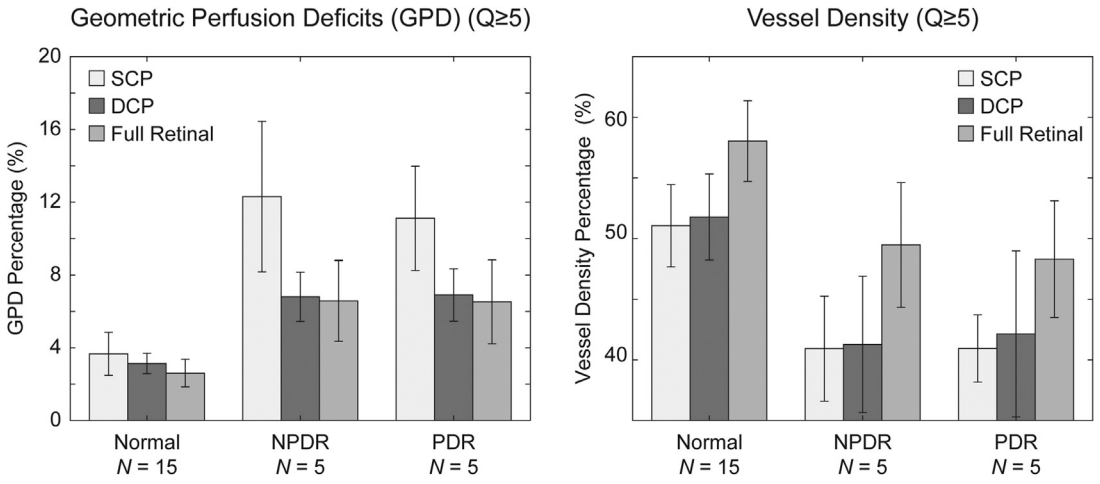

FIGURE 5. Bar plot show GPD percentages and vessel density percentages calculated using SCP, DCP, and full retinal OCTA projections, respectively. Eyes are subdivided into 3 groups: normal, NPDR, and PDR. Only 3 × 3 mm^2 macular OCTA scans with quality index, Q ≥ 5, are included. DCP = deep capillary plexus; GPD = geometric perfusion deficit; NPDR = nonproliferative diabetic retinopathy; PDR proliferative diabetic retinopathy; OCTA = optical coherence tomography angiography; SCP = superficial capillary plexus.

TABLE 5. GPD Percentage, Vessel Density Percentage, and Statistical Significance (*P* values) for Differentiating Normal Eyes and Eyes with Diabetic Retinopathy (3 × 3-mm^2 Macular OCTA Scans with Quality Index ≥5 Only)

	GPDs			Vessel Density		
	SCP	DCP	Full Retinal	SCP	DCP	Full Retinal
Percentage[a]						
Normal (n = 15)	3.7 ± 1.2	3.1 ± 0.6	2.6 ± 0.8	51.1 ± 3.4	51.8 ± 3.5	58.0 ± 3.3
NPDR (n = 5)	12.3 ± 4.1	6.8 ± 1.4	6.6 ± 2.2	40.9 ± 4.3	41.3 ± 5.6	49.5 ± 5.1
PDR (n = 5)	11.1 ± 2.9	6.9 ± 1.4	6.5 ± 2.3	40.9 ± 2.8	42.1 ± 6.8	48.3 ± 4.8
P value[b]						
Normal vs. NPDR	.002	.003	.003	.006	.007	.03
Normal vs. PDR	.005	.003	.004	.005	.02	.006
NPDR vs. PDR	1.00	1.00	1.00	1.00	1.00	1.00

DCP = deep capillary plexus; GPD = geometric perfusion deficit; NPDR = nonproliferative diabetic retinopathy; OCTA = optical coherence tomography angiography; PDR = proliferative diabetic retinopathy; SCP = superficial capillary plexus.

[a]Data are mean ± standard deviation.

[b]Significance level is $P < .05$. *P* values were calculated using Kruskal-Wallis 1-way ANOVA on ranks and post hoc Dunn tests corrected for multiple comparison ($m = 3$).

among the groups as their 3 × 3-mm^2 counterparts. Table 9 summarizes the respective intergroup statistics. In all 3 subregions, GPD percentages were significantly higher in NPDR and DR eyes, whereas vessel density percentages were significantly lower.

DISCUSSION

MACULAR ISCHEMIA IS A KEY DRIVER OF DR PROGRESSION,[2,35,36] and numerous studies have aimed at quantifying vascular remodeling for diagnosis and predicting progression. Notable early investigations using OCTA include studies by Jia and associates[14] and Hwang and associates,[15] in which low OCTA signals in macular OCTA images were detected and interpreted as areas of retinal capillary nonperfusion. Both studies indicated DR eyes were associated with increased total capillary nonperfusion areas.[14,15] In another early study, Agemy and associates[8] proposed a vascular topographic metric, perfusion density, for grading of DR severity. Using segmented OCTA images, they found a trend of decreasing perfusion density with increasing DR severity. Similar results were reported by other groups using various vessel density-derived methods.[9–11]

TABLE 6. Sum of 10 and 20 Largest GPD Areas in 3 × 3-mm^2 Macular OCTA

	10 Largest GPD Areas			20 Largest GPD Areas		
Group[a]	SCP	DCP	Full Retinal	SCP	DCP	Full Retinal
Normal (n = 15)	0.06 ± 0.02	0.04 ± 0.01	0.05 ± 0.02	0.09 ± 0.03	0.07 ± 0.02	0.07 ± 0.03
NPDR (n = 6)	0.26 ± 0.11	0.09 ± 0.03	0.11 ± 0.05	0.37 ± 0.16	0.14 ± 0.04	0.16 ± 0.07
PDR (n = 6)	0.23 ± 0.08	0.12 ± 0.07	0.13 ± 0.08	0.33 ± 0.11	0.16 ± 0.08	0.18 ± 0.09

DCP = deep capillary plexus; GPD = geometric perfusion deficits; NPDR = nonproliferative diabetic retinopathy; OCTA = optical coherence tomography angiography; PDR = proliferative diabetic retinopathy; SCP = superficial capillary plexus.

[a]Data are mean ± standard deviation in mm^2.

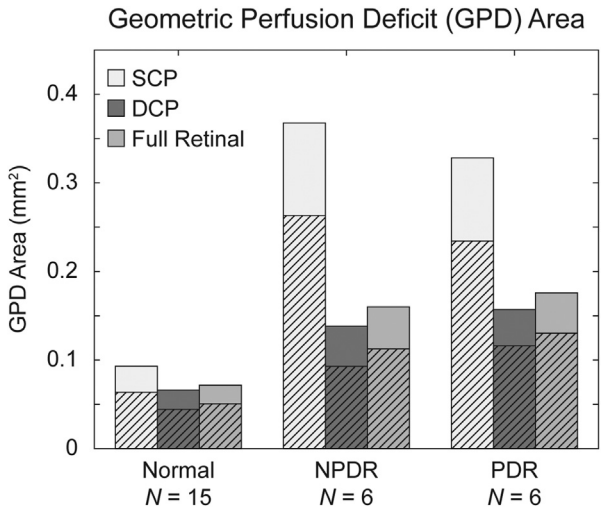

FIGURE 6. Focal changes are represented by the sum of the largest GPD areas, calculated using all 3 × 3-mm^2 macular OCTA scans. Shaded area indicates sum of 10 largest GPD areas. Full height indicates sum of 20 largest GPD areas. DCP = deep capillary plexus; GPD = geometric perfusion deficit; NPDR = nonproliferative diabetic retinopathy; OCTA = optical coherence tomography angiography; PDR = proliverative diabetic retinopathy; SCP = superficial capillary plexus

TABLE 7. Statistical Significance (*P* values) for Differentiating Normal Eyes and Eyes with Diabetic Retinopathy Using Focal GPD Areas (All 3 × 3-mm^2 Macular OCTA Scans)

	10 Largest GPD Areas			20 Largest GPD Areas		
Comparison[a]	SCP	DCP	Full Retinal	SCP	DCP	Full Retinal
Normal vs. NPDR	< .001	.005	.006	.001	.003	.007
Normal vs. PDR	.003	.005	.004	.004	.005	.002
NPDR vs. PDR	1.00	1.00	1.00	1.00	1.00	1.00

DCP = deep capillary plexus; GPD = geometric perfusion deficits; NPDR = nonproliferative diabetic retinopathy; OCTA = optical coherence tomography angiography; PDR = proliferative diabetic retinopathy; SCP = superficial capillary plexus.

[a]Significance level is $P < .05$. *P* values were calculated using Kruskal-Wallis 1-way ANOVA on ranks and post hoc Dunn tests corrected for multiple comparisons ($m = 3$).

More recently, approaches that automatically characterized vascular features, such as intercapillary areas, have gained interest.[16,17] For example, Krawiz and associates[16] used an eccentricity-based normative database and thresholding to detect regions with pathological intercapillary areas. In addition to showing similar trends to vessel density studies, the parafoveal intercapillary area metric showed promising diagnostic potential, with an area under the curve (AUC) over 0.8 from the receiver operating characteristic (ROC) curve differentiating eyes without clinical retinopathy from all DR eyes.

The present study develops the concept of geometric perfusion deficits, a metric that is related to the underlying physiology of oxygen diffusion and ischemia. By using physiological principles, the GPD metric facilitates clinical interpretation and potentially eliminates the need for normative databases. This study found that GPD percentage was significantly higher in NPDR and PDR eyes than in normal eyes. Moreover, GPD percentage had a strong negative correlation with vessel density percentage, suggesting the 2 metrics are inversely related. The high correlation further suggests that GPD percentage is also correlated with disease severity in a manner similar to vessel density percentage.[8–11] Unfortunately, due to the small sample size, this hypothesis could not be tested explicitly. This study also used GPD to investigate focal vascular alterations in DR eyes. Using the sum of the 10 and 20 largest GPD areas, it was found this focal marker performed comparably to the global GPD percentage metric. This strongly supports the fact that GPD is sensitive to focal lesions. In contrast, analysis of focal lesions using vessel density percentage requires that a threshold level be empirically selected or derived relative to a normative database, complicating the analysis. One strength of this study is that repeated OCTA imaging data enabled evaluation of the test-retest repeatability of the GPD and vessel density percentage metrics. Notably, the vessel density percentage statistics agree with prior

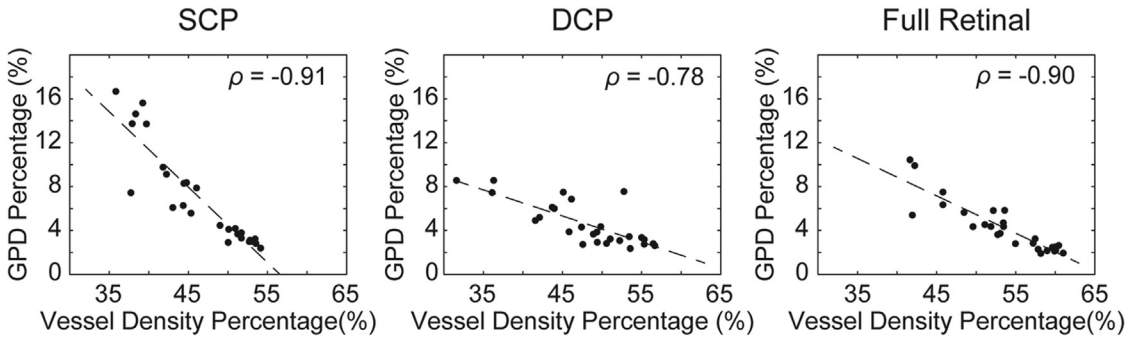

FIGURE 7. Correlation between the GPD percentages and vessel density percentages, calculated using all 3 × 3-mm^2 macular OCTA scans. Dashed line indicates linear regression; ρ = Pearson correlation coefficient; DCP = deep capillary plexus; GPD = geometric perfusion deficit; OCTA = optical coherence tomography angiography; SCP = superficial capillary plexus.

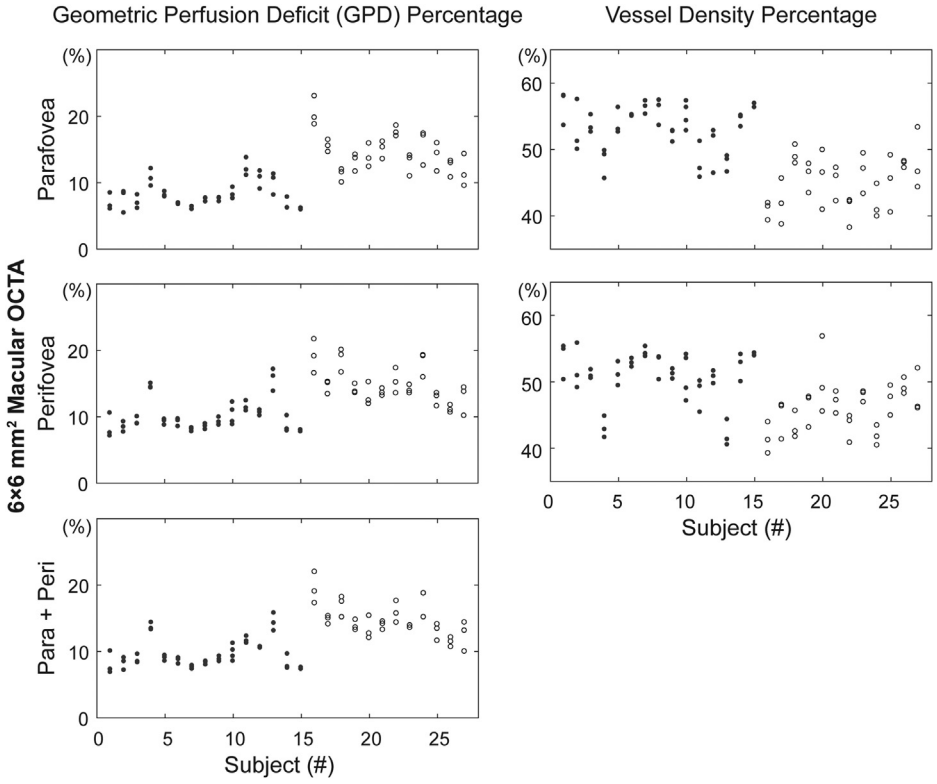

FIGURE 8. Scatter plots show repeated measurements of GPD percentages and vessel density percentages for each subject using the SCP OCTA projection from 6 × 6-mm^2 macular scans. The GPD and vessel density percentages were calculated, respectively, on 3 subregions: the parafovea, that is, between the 1- and 3-mm-diameter ETDRS circle; the perifoveal, that is, between the 3- and 6-mm-diameter ETDRS circle; and the combined para- and perifovea, that is, between the 1- and 6-mm ETDRS circle. Vessel density percentages in the combined para- and perifoveal regions were not available in the Optovue software and are not shown. Filled circles = normal eyes; open circles = eyes diagnosed with diabetic retinopathy. ETDRS = Early Treatment Diabetic Retinopathy Study; GPD = geometric perfusion deficit; OCTA = optical coherence tomography angiography; SCP = superficial capillary plexus.

analyses,[8,37] and our GPD percentage showed improved repeatability compared to vessel density percentage in the majority of cases.

The GPD model was used to identify both global and focal ischemia within the inner retina. Ischemia can activate hypoxia-inducible factors and the subsequent expression of VEGF.[3,38,39] Pathological VEGF concentrations disrupt the tight junction of the blood-retina barrier causing leakage of plasma (ie, DME) and, progressively, retinal neovascularization (ie, PDR). Thus, identifying

TABLE 8. Mean and Median SD of Repeated Measurements for GPD and Vessel Density Percentages Using the Superficial Capillary Plexus OCTA Projection from 6 × 6-mm^2 Macular Scans

		GPD Percentage		Vessel Density Percentage		*P* Value[a]
Group	Region	Mean SD	Median SD	Mean SD	Median SD	(*U* test)
Normal	Parafovea	0.87	0.93	1.82	2.00	0.02
	Perifovea	0.79	0.60	1.72	1.80	0.005
	Para + Peri	0.69	0.54	-	-	-
DR	Parafovea	1.65	1.53	2.77	2.61	0.02
	Perifovea	1.40	1.40	2.40	2.20	0.03
	Para + Peri	1.33	1.44	-	-	-

DR = diabetic retinopathy; GPD = geometric perfusion deficits; OCTA = optical coherence tomography angiography; Para + Peri = parafoveal plus perifoveal; SD = standard deviation.

[a]Significance level is $P < .05$. Wilcoxon rank-sum significance test (*U* test) was used to compare the median standard deviations of the geometric perfusion deficit and vessel density percentages.

TABLE 9. GPD Percentage, Vessel Density Percentage, and Statistical Significance (*P* values) for Differentiating Normal Eyes and Eyes with Diabetic Retinopathy (All 6 × 6-mm^2 Macular Superficial Capillary Plexus OCTA)

	GPDs			Vessel Density	
	Parafovea	Perifovea	Para+Peri	Parafovea	Perifovea
Percentage[a]					
Normal (n = 15)	8.1 ± 1.9	10.0 ± 2.3	9.5 ± 2.1	53.2 ± 3.1	50.7 ± 3.6
NPDR (n = 6)	14.6 ± 3.7	15.5 ± 2.8	15.3 ± 2.6	45.2 ± 3.6	45.7 ± 3.5
PDR (n = 6)	14.3 ± 1.4	14.0 ± 2.3	14.1 ± 2.0	44.6 ± 2.3	46.0 ± 2.5
P value[b]					
Normal vs. NPDR	.003	.005	.004	.006	.02
Normal vs. PDR	<.001	.04	.01	.001	.02
NPDR vs. PDR	1.00	1.00	1.00	1.00	1.00

GPD = geometric perfusion deficits; NPDR = nonproliferative diabetic retinopathy; OCTA = optical coherence tomography angiography; Para+Peri = parafoveal plus perifoveal; PDR = proliferative diabetic retinopathy.

[a]Data are mean ± standard deviation.

[b]Significance level is $P < .05$. *P* values were calculated using Kruskal-Wallis 1-way ANOVA on ranks and post hoc Dunn tests corrected for multiple comparison ($m = 3$).

retinal ischemia is crucial for understanding and managing DR pathogenesis. Although this GPD metric only provides an indirect estimation, its high test-retest repeatability and sensitivity to focal lesions can potentially bring more granularity in the investigation of hypoxia and DR associations. Most importantly, GPD analysis uses OCTA scans that are readily available from commercial instruments, offering great accessibility compared with retinal oximetry approaches.[40–42] Potential applications include cross-sectional studies that correlate locations of hypoxic regions, DME, and neovascularization, as well as longitudinal studies that investigate DR progression and treatment response.

It is interesting to consider the open question of whether DCP OCTA is better suited than SCP OCTA for quantifying DR-related vascular remodeling. For example, Agemy and associates[8] and Al-Sheikh and associates[9] independently published study results that favored DCP and SCP OCTA, respectively. The present study, although limited in its cohort size and statistical power, is consistent with the notion that SCP better differentiates DR eyes from normal eyes when using GPD percentage and vessel density percentage metrics. The authors hypothesize that this finding is in part attributable to OCT beam attenuation, which causes a lower OCT signal in the DCP than the SCP. In addition to reducing OCTA quality, lower OCT signals also complicate segmentation. This hypothesis is supported by the observation that when we repeated our analysis using only higher quality OCTA images (quality index ≥5), the difference in DCP vessel density percentage between normal and PDR eyes became statistically significant. However, it is also possible that the high prevalence of DME in the present cohort might have confounded DCP analysis.[9,43] Thus, a larger NPDR and PDR category with a

balanced number of eyes with and without DME would be necessary to investigate the role of the DCP during DR progression.

Most of the present quantitative analysis and statistical tests were performed using 3 × 3-mm^2 macular OCTA scans. In contrast, only the SCP projection from 6 × 6-mm^2 macular OCTA scans was included for calculating GPD and vessel density percentages between normal and DR eyes. This is because the smaller 3 × 3-mm^2 field of view has better A-scan sampling density and overall quality than larger 6 × 6-mm^2 fields of view. For the same reason, the authors refrained from directly comparing the performance of 3 × 3-mm^2 versus that of 6 × 6-mm^2 scans. It is worthwhile noting that current studies suggest that the peripheral retina is first affected in DR and can better predict disease progression.[44] This indicates that even larger fields of view can be of more clinical utility than smaller ones. However, at the same time, other factors which are not related to pathology and which unfortunately were not controlled in this study, can confound comparisons.[43] Indeed, it was found that quantitative OCTA metrics were susceptible to low-quality scans. However, as faster, higher performance OCTA instruments become available, larger field-of-view OCTA scans will achieve quality comparable to existing 3 × 3-mm^2 scans, enabling a more accurate investigation of the macula versus peripheral retina.

The limitations of our capillary perfusion model merit further discussion. First, the proposed GPD metric only measures perfusion deficits caused by abnormalities in vessel geometry. While the spatial distribution of retinal capillaries is one factor determining oxygen concentration of retinal tissue, other factors, such as the partial pressure of oxygen in the supplying capillaries and the metabolic activity of the tissue, which are not measured by standard OCTA, also contribute. Moreover, our geometric diffusion model only incorporated 2D diffusion, which assesses oxygen diffusion in the en face plane defined by the OCTA projection (ie, within the SCP, DCP, or total retinal OCTA projection), effectively ignoring oxygen diffusion along the axial direction. Although this is clearly an approximation of the true physiological oxygen diffusion, the 2D model was chosen because of the challenges in 3-D OCTA analysis. Particularly, 3D OCTA analysis is complicated by i) OCTA projection artifacts[45]; ii) increased noise, because the OCTA signal is not averaged as it is in an en face projection; and iii), variations in the oxygen metabolic rate of retinal cell types and layers. However, it is worth noting that these GPD metrics naturally extend to 3D, assuming that 3D vessel geometry can be extracted from OCTA data. This contrasts with previously proposed intercapillary area metrics, which do not have obvious 3-D analogues.

A single, fixed threshold of 30 μm was used to demarcate perfusion deficit regions. This threshold was based on measurements of intercapillary distance made using laser Doppler flowmetry, adaptive optics scanning laser ophthalmoscopy, and OCTA.[16,28,29] As noted in these studies, the SCP directly bordering the FAZ is single layered and, therefore, should offer a reasonable approximation to the optimal diffusion in normal subjects.[16,46,47] However, when assessing larger fields of view, an eccentric dependent threshold, rather than a single value, may be preferable.

This study was also limited by its retrospective design and limited cohort size, preempting our ability to perform subgroup analysis of mild, moderate, and severe NPDR eyes, as well as eyes with and without DME. Such subgroup analysis would help assess the suitability of GPD analysis for monitoring NPDR progression and stratifying patients for treatment. Separating eyes on the basis of DME status would be particularly interesting in light of the finding that DME eyes have reduced total retinal blood flow compared to eyes without DME.[9,48]

In conclusion, GPD, a novel marker of oxygen diffusion computed from OCTA-derived microvascular geometry, was developed and GPD percentages were used to study microvascular remodeling in DR. Using multiple repeated OCTA acquisitions, the test-retest repeatability of global GPD percentage metrics was evaluated, and compared against existing vessel density percentage metrics. Results show that GPD percentages have good test-retest repeatability and are more robust to vessel discontinuities than intercapillary area metrics. Moreover, statistical analysis suggested that GPD percentages can serve as a biomarker to differentiate between normal and DR eyes. Most importantly, GPD physiological interpretability can facilitate clinical interpretation of the metric and allow more intuitive comparison between patients.

ALL AUTHORS HAVE COMPLETED AND SUBMITTED THE ICMJE FORM FOR DISCLOSURE OF POTENTIAL CONFLICTS OF INTEREST and none were reported. This work was supported by US National Institutes of Health grants R01-EY011289 and R01-EY029058; a Beckman-Argyros Award in Vision Research; an unrestricted grant from Research to Prevent Blindness; an António Champalimaud Vision Award; a Retina Research Foundation Award; and Topcon Corp.

L.M.Z. has received research support and research equipment from Heidelberg Engineering, Carl Zeiss Meditec, Optovue and Topcon. R.N.W. has received instruments for research from Optovue, Carl Zeiss Meditec, and Heidelberg Engineering.

J.G.F. has financial interests in and intellectual property licensed to Optovue, Carl Zeiss Meditec; and has received research support from Topcon. The study presents data acquired with Optovue instruments, however, Optovue did not participate in the analysis of study results or preparation of the manuscript.

REFERENCES

1. Hammes H-P, Lin J, Renner O, et al. Pericytes and the pathogenesis of diabetic retinopathy. *Diabetes* 2002;51(10):3107–3112.
2. Frank RN. Diabetic retinopathy. *N Engl J Med* 2004;350(1):48–58.
3. Aiello LP, Avery RL, Arrigg PG, et al. Vascular endothelial growth factor in ocular fluid of patients with diabetic retinopathy and other retinal disorders. *N Engl J Med* 1994;331(22):1480–1487.
4. Early Treatment Diabetic Retinopathy Study Research Group. Classification of diabetic retinopathy from fluorescein angiograms: ETDRS report number 11. *Ophthalmology* 1991;98(5, Supplement):807–822.
5. Conrath J, Giorgi R, Raccah D, Ridings B. Foveal avascular zone in diabetic retinopathy: quantitative vs qualitative assessment. *Eye* 2005;19(3):322–326.
6. Kashani AH, Chen C-L, Gahm JK, et al. Optical coherence tomography angiography: a comprehensive review of current methods and clinical applications. *Prog Retin Eye Res* 2017;60:66–100.
7. Spaide RF, Fujimoto JG, Waheed NK, Sadda SR, Staurenghi G. Optical coherence tomography angiography. *Prog Retin Eye Res* 2018;64:1–55.
8. Agemy SA, Scripsema NK, Shah CM, et al. Retinal vascular perfusion density mapping using optical coherence tomography angiography in normals and diabetic retinopathy patients. *Retina* 2015;35(11):2353–2363.
9. Al-Sheikh M, Akil H, Pfau M, Sadda SR. Swept-source oct angiography imaging of the foveal avascular zone and macular capillary network density in diabetic retinopathy. *Invest Ophthalmol Vis Sci* 2016;57(8):3907–3913.
10. Kim AY, Chu Z, Shahidzadeh A, Wang RK, Puliafito CA, Kashani AH. Quantifying microvascular density and morphology in diabetic retinopathy using spectral-domain optical coherence tomography. *Invest Ophthalmol Vis Sci* 2016;57(9):OCT362–OCT370.
11. Samara WA, Shahlaee A, Adam MK, et al. Quantification of diabetic macular ischemia using optical coherence tomography angiography and its relationship with visual acuity. *Ophthalmology* 2017;124(2):235–244.
12. Dupas B, Minvielle W, Bonnin S, et al. Association between vessel density and visual acuity in patients with diabetic retinopathy and poorly controlled type 1 diabetes. *JAMA Ophthalmol* 2018;136(7):721–728.
13. Ishibazawa A, Nagaoka T, Takahashi A, et al. Optical coherence tomography angiography in diabetic retinopathy: a prospective pilot study. *Am J Ophthalmol* 2015;160(1):35–44.
14. Jia Y, Bailey ST, Hwang TS, et al. Quantitative optical coherence tomography angiography of vascular abnormalities in the living human eye. *Proc Natl Acad Sci U S A* 2015;112(18):E2395–E2402.
15. Hwang TS, Gao SS, Liu L, et al. Automated quantification of capillary nonperfusion using optical coherence tomography angiography in diabetic retinopathy. *JAMA Ophthalmol* 2016;134(4):367–373.
16. Krawitz BD, Phillips E, Bavier RD, et al. Parafoveal nonperfusion analysis in diabetic retinopathy using optical coherence tomography angiography. *Transl Vis Sci Technol* 2018;7(4):4.
17. Schottenhamml J, Moult EM, Ploner S, et al. An automatic, intercapillary area-based algorithm for quantifying diabetes-related capillary dropout using optical coherence tomography angiography. *Retina* 2016;36:S93–S101.
18. Uji A, Balasubramanian S, Lei J, Baghdasaryan E, Al-Sheikh M, Sadda SR. Impact of multiple en face image averaging on quantitative assessment from optical coherence tomography angiography images. *Ophthalmology* 2017;124(7):944–952.
19. Early Treatment Diabetic Retinopathy Study Research Group. Grading diabetic retinopathy from stereoscopic color fundus photographs—an extension of the modified Airlie House classification: ETDRS report number 10. *Ophthalmology* 1991;98(Suppl 5):786–806.
20. Kraus MF, Potsaid B, Mayer MA, et al. Motion correction in optical coherence tomography volumes on a per a-scan basis using orthogonal scan patterns. *Biomed Opt Express* 2012;3(6):1182–1199.
21. Kraus MF, Liu JJ, Schottenhamml J, et al. Quantitative 3D-OCT motion correction with tilt and illumination correction, robust similarity measure and regularization. *Biomed Opt Express* 2014;5(8):2591–2613.
22. Camino A, Zhang M, Gao SS, et al. Evaluation of artifact reduction in optical coherence tomography angiography with real-time tracking and motion correction technology. *Biomed Opt Express* 2016;7(10):3905–3915.
23. Linsenmeier RA, Braun RD. Oxygen distribution and consumption in the cat retina during normoxia and hypoxemia. *J Gen Physiol* 1992;99(2):177–197.
24. Ahmed J, Braun RD, Dunn R Jr, Linsenmeier RA. Oxygen distribution in the macaque *Retina*. *Invest Ophthalmol Vis Sci* 1993;34(3):516–521.
25. Lau JCM, Linsenmeier RA. Oxygen consumption and distribution in the long-evans rat Retina. *Exp Eye Res* 2012;102:50–58.
26. Yi J, Liu W, Chen S, et al. Visible light optical coherence tomography measures retinal oxygen metabolic response to systemic oxygenation. *Light Sci Appl* 2015;4(9):e334.
27. Frangi AF, Niessen WJ, Vincken KL, Viergever MA. Multiscale Vessel Enhancement Filtering; 1998. Heidelberg.
28. Chui TYP, Gast TJ, Burns SA. Imaging of vascular wall fine structure in the human retina using adaptive optics scanning laser ophthalmoscopy. *Invest Ophthalmol Vis Sci* 2013;54(10):7115–7124.
29. Jumar A, Harazny JM, Ott C, et al. Retinal capillary rarefaction in patients with type 2 diabetes mellitus. *PLoS One* 2016;11(12):e0162608.
30. Bresnick GH, Condit R, Syrjala S, Palta M, Groo A, Korth K. Abnormalities of the foveal avascular zone in diabetic retinopathy. *JAMA Ophthalmol* 1984;102(9):1286–1293.
31. Takase N, Nozaki M, Kato A, Ozeki H, Yoshida M, Ogura Y. Enlargement of foveal avascular zone in diabetic eyes evaluated by en face optical coherence tomography angiography. *Retina* 2015;35(11):2377–2383.
32. Salz DA, de Carlo TE, Adhi M, et al. Select features of diabetic retinopathy on swept-source optical coherence tomographic angiography compared with fluorescein angiography and normal eyes. *JAMA Ophthalmol* 2016;134(6):644–650.

33. Koo TK, Li MY. A guideline of selecting and reporting intraclass correlation coefficients for reliability research. *J Chiropr Med* 2016;15(2):155–163.
34. Dunn OJ. Multiple comparisons among means. *J Am Stat Assoc* 1961;56(293):52–64.
35. Klein R, Klein BEK, Moss SE. Visual impairment in diabetes. *Ophthalmology* 1984;91(1):1–9.
36. Sim DA, Keane PA, Zarranz-Ventura J, et al. The effects of macular ischemia on visual acuity in diabetic retinopathy. *Invest Ophthalmol Vis Sci* 2013;54(3):2353–2360.
37. You Q, Freeman WR, Weinreb RN, et al. Reproducibility of vessel density measurement with optical coherence tomography angiography in eyes with and without retinopathy. *Retina* 2017;37(8):1475–1482.
38. Simó R, Hernández C. Intravitreous anti-VEGF for diabetic retinopathy: hopes and fears for a new therapeutic strategy. *Diabetologia* 2008;51(9):1574.
39. Nicholson BP, Schachat AP. A review of clinical trials of anti-VEGF agents for diabetic retinopathy. *Graefes Arch Clin Exp Ophthalmol* 2010;248(7):915–930.
40. Harris A, Dinn RB, Kagemann L, Rechtman E. A review of methods for human retinal oximetry. ophthalmic surg lasers imaging. *Retina* 2003;34(2):152–164.
41. Chen S, Shu X, Nesper PL, Liu W, Fawzi AA, Zhang HF. Retinal oximetry in humans using visible-light optical coherence tomography. *Biomed Opt Express* 2017;8(3):1415–1429.
42. Chong SP, Bernucci M, Radhakrishnan H, Srinivasan VJ. Structural and functional human retinal imaging with a fiber-based visible light OCT ophthalmoscope. *Biomed Opt Express* 2017;8(1):323–337.
43. Hirano T, Kitahara J, Toriyama Y, Kasamatsu H, Murata T, Sadda S. Quantifying vascular density and morphology using different swept-source optical coherence tomography angiographic scan patterns in diabetic retinopathy. *Br J Ophthalmol* 2019;103(2):216–221.
44. Silva PS, Cavallerano JD, Haddad NMN, et al. Peripheral lesions identified on ultrawide field imaging predict increased risk of diabetic retinopathy progression over 4 years. *Ophthalmology* 2015;122(5):949–956.
45. Spaide RF, Fujimoto JG, Waheed NK. Image artifacts in optical coherence tomography angiography. *Retina* 2015; 35(11):2163–2180.
46. Iwasaki M, Inomata H. Relation between superficial capillaries and foveal structures in the human retina. *Invest Ophthalmol Vis Sci* 1986;27(12):1698–1705.
47. Bek T, Jensen PK. Three-dimensional structure of human retinal vessels studied by vascular casting. *Acta Ophthalmol (Copenh)* 1993;71(4):506–513.
48. Lee B, Novais EA, Waheed NK, et al. En face doppler optical coherence tomography measurement of total retinal blood flow in diabetic retinopathy and diabetic macular edema. *JAMA Ophthalmol* 2017;135(3):244–251.